Electronic Supplementary Material (ESI) for Sustainable Energy & Fuels.

Supporting Information

Effective inter-chain charge transfer and high charge mobility in polymeric carbon nitride arising from controllable molecular structure for enhanced photocatalytic H_2O_2 and H_2 production

Zonglin Li,[1] Qing Yang,[1] Hui Zhang,[*] Fukai Zheng, Yonghai Wang, Jianhua Sun[*]

School of Chemistry and Chemical Engineering, Institute of Advanced Functional Materials for Energy, Jiangsu University of Technology, Changzhou 213001, Jiangsu Province, P. R. China

[1] *These authors contributed equally to this work and should be considered co-first authors.*

*Corresponding authors.

E-mail address: zhanghui@jsut.edu.cn (H. Zhang); sunjh@jsut.edu.cn (J. Sun).

Characterization: X-ray diffraction (XRD) patterns were obtained from a X-Pert Powder X-ray diffractometer (PANalytical). Elemental analysis (EA) was carried out on a UNICUBE element analyzer. Scanning electron microscopy (SEM) images were collected on a Hitachi S-3400N microscopy. Transmission electron microscopy (TEM) characterization was performed on a JEM-2100 instrument at an acceleration voltage of 200 kV. Fourier transform infrared (FT-IR) spectra were measured on a Thermo Nicolet iS10 spectrometer. N_2 adsorption-desorption isotherms were obtained on a Micromeritics ASAP 2020 instrument. X-ray photoelectron spectroscopy (XPS) measurements were conducted on a Thermo Fisher ESCALAB Xi+ spectrometer with monochromic Al Kα X-ray. UV-vis diffuse reflection spectra (DRS) were recorded on a Perkinelmer Lambda 850+ spectrophotometer. Steady-state and time-resolved photoluminescence (PL) spectra were measured on a FluoroMax+ spectrophotometer (HORIBA). Electron spin resonance (ESR) spectra were recorded on a Bruker MicroESR spectrometer.

The details of the concentrated sulfuric acid treatment: The mixture of 200 mg BCN and 2.00 mL H_2SO_4 was stirred at 100 ℃ for 1 h. Then the mixture gradually turned into a pale yellow solution. The PTI and CN-*x* (*x* = 70%, 80%, 90%, 100%) samples were treated with H_2SO_4 under the same condition.

Photocatalytic H_2O_2 production: The photocatalytic reduction of O_2 to H_2O_2 was performed in a top-irradiation reaction vessel. Typically, 50 mg prepared photocatalyst was dispersed in the mixture of 90 mL deionized water and 10 mL ethanol. The suspension solutions were stirred for 30 min in the dark with continually O_2 bubbling to reach the absorption-desorption equilibrium. Then the solutions were exposed to visible light provided by a 300 W Xe lamp with a 420 nm cut-off filter. A continuous magnetic stirrer and cooling water were applied during the experiment. During the irradiation, ~2 mL solution was sampled every 15 min and filtrated with a 0.45 μm filter to remove the photocatalyst.

The amount of H_2O_2 was analyzed by colorimetric method using horseradish peroxidase (HRP)/3,3',5,5'-tetramethylbenzidine (TMB) system. HRP is used to catalyze TMB in the presence of H_2O_2 to produce chromogenic reaction. Typically, 2

mL Na_2HPO_4/NaH_2PO_4 (0.1 M, pH 7.4) buffer, 10 μL TMB (0.1 M), and 10 μL HRP (0.1 M) were added to 100 μL filtration from reaction solution. After 10 min, the solution was blue. Then 200 μL H_2SO_4 (3 M) was added to stop the reaction, giving rise to a yellow product that corresponds to oxidation of TMB. The amount of oxidation product formed was quantified spectrophotometrically at 450 nm (The solution was diluted before UV-vis absorption measurement if necessary), from which the amount of H_2O_2 produced during each reaction was estimated. Fig. S2 shows the linear fitting spectra for the H_2O_2 standard solution.

The apparent quantum efficiency (AQE) for H_2O_2 production was measured by replacing the cut-off filter with corresponding band-pass filter. The AQE is calculated from the following equation:

$$\text{AQE} = \frac{2 \times \text{number of evolved H2O2 molecules}}{\text{the number of incident photos}} \times 100\%$$

Further, the number of evolved H_2O_2 molecules can be expressed as:

$$\text{the number of evolved } H_2O_2 \text{ molecules} = n(H_2O_2) \cdot N_A$$

And the number of incident photons can be expressed as:

$$\text{the number of incident photons} = \frac{E \times \lambda}{h \times c} = \frac{P \times S \times t \times \lambda}{h \times c}$$

Where $n(H_2O_2)$ refers to the H_2O_2 production (mol), N_A is the Avogadro constant (6.022×10^{23} mol^{-1}); E refers to the total energy of the incident photon (J), λ is the wavelength of incident light (m), h is the Planck constant (6.626×10^{-34} J·s), c is the light speed (3×10^{8} $m\cdot s^{-1}$), P refers to the average spectral irradiance ($W\cdot cm^{-2}$), S is the irradiation area (27.34 cm^2 in this paper), and t is the irradiation time (3600 s in this paper). By integrating above formulas, the AQE is obtained as follows:

$$\text{AQE} = \frac{2 \times n(H_2O_2) \cdot N_A \times h \times c}{P \times S \times t \times \lambda} \times 100\%$$

The measured values of $n(H_2O_2)$ and P are listed in Table S1:

Table S1 The measured data and corresponding AQE

λ / 10^{-9} (m)	$n(H_2O_2)$ / 10^{-6} (mol)	P / 10^{-3} ($W\cdot cm^{-2}$)[a]	AQE (%)

380	105	0.993	67.7
420	85.5	0.875	56.6
450	142	2.85	26.9
475	20.0	3.93	2.61
500	4.72	2.05	1.12

[a] The average intensity of irradiation was measurd by a Newport Oriel 91150V reference cell.

For example, the AQE at 420 nm is calculated as follows:

$$AQE = \frac{2 \times n(H_2O_2) \cdot N_A \times h \times c}{P \times S \times t \times \lambda} \times 100\%$$

$$= \frac{2 \times 85.5 \times 10 - 6 \times 6.022 \times 1023 \times 6.626 \times 10 - 34 \times 3 \times 108}{0.875 \times 10 - 3 \times 27.34 \times 3600 \times 420 \times 10 - 9} \times 100\%$$

$$= 56.6\%$$

Photocatalytic H_2 production: The photocatalytic hydrogen production reactions were carried out in a top-irradiation reaction vessel connected to a glass closed system. Typically, 50 mg prepared photocatalyst was dispersed in the mixture of 90 mL deionized water and 10 mL triethanolamine (TEOA). Then, 3 wt% H_2PtCl_6 (based on Pt) as the precursor of cocatalyst Pt was added. After degassed under vacuum to completely remove air, the reaction solution was irradiated by a 300 W Xe-lamp with a cut-off filter ($\lambda > 420$ nm). During the irradiation, the reaction temperature was maintained at 15 ℃ by cycle water. The generated H_2 was analyzed by an on-line gas chromatography (GC-7900, thermal conductive detector, 5 Å molecular sieve column), using Ar as the carrier.

The AQE for H_2 evolution was measured by replacing the cut-off filter with corresponding band-pass filter. The AQE is calculated from the following equation:

$$AQE = \frac{2 \times \text{number of evolved } H_2 \text{ molecules}}{\text{the number of incident photos}} \times 100\%$$

Electrochemical and photoelectrochemical measurements: Rotating disk electrode

(RDE) measurements was conducted on a CHI-760E workstation (CH Instruments) coupled with a rotating disk electrode system. The three-electrode cell system was consisting of a Ag/AgCl electrode as the reference electrode and a Pt wire as the counter electrode. The working electrode was prepared as follows: 5 mg photocatalysts was dispersed in 0.5 mL ethanol containing 0.02 % Nafion by ultrasonication. The slurry (6 μL) was put onto a disk electrode and dried at room temperature. The linear sweep voltammogram (LSV) were obtained in an O_2-saturated 0.1 M KOH with a scan rate 2 mV s^{-1}. The average transfer electron number (n) in the O_2 reduction was obtained by the slopes of Koutecky-Levich plots with the following equation:

$$J^{-1} = J_k^{-1} + B^{-1}\omega^{-1/2}$$

$$B = 0.2nFv^{-1/6}C_0D_0^{2/3}$$

where J, J_k and ω are the tested current density, kinetic current density and rotating speed (rpm), respectively. F and v are the Faraday constant (96485 C mol^{-1}) and kinetic viscosity of water (0.01 cm^2 s^{-1}), C_0 and D_0 are the bulk concentration of O_2 in water (1.2×10^{-3} mol L^{-1}) and the diffusion coefficient of O_2 (1.9×10^{-5} cm^2 s^{-1}).

Mott-Schottky plots, electrochemical impedance spectra (EIS), and photocurrent were all performed by CHI-760E workstation (CH Instruments) in a standard three-electrode system using the prepared samples as the working electrodes, Ag/AgCl electrode as a reference electrode, and a Pt wire as the counter electrode. The electrolyte was 0.2 M Na_2SO_4 aqueous solution. The working electrodes were prepared as follows: ~5 mg sample was dispersed in 0.02 wt% Nafion solution to afford a suspension. The suspension was sonicated for 1 h and then spread on to a 1.0 cm × 1.0 cm exposed ITO glass, dried in the air. The Mott-Schottky plots were measured at frequencies of 3500 Hz. The photocurrent was measured under -0.3 V bias voltage and the light source was a 300 W Xe-lamp with a cut-off filter (λ > 420 nm).

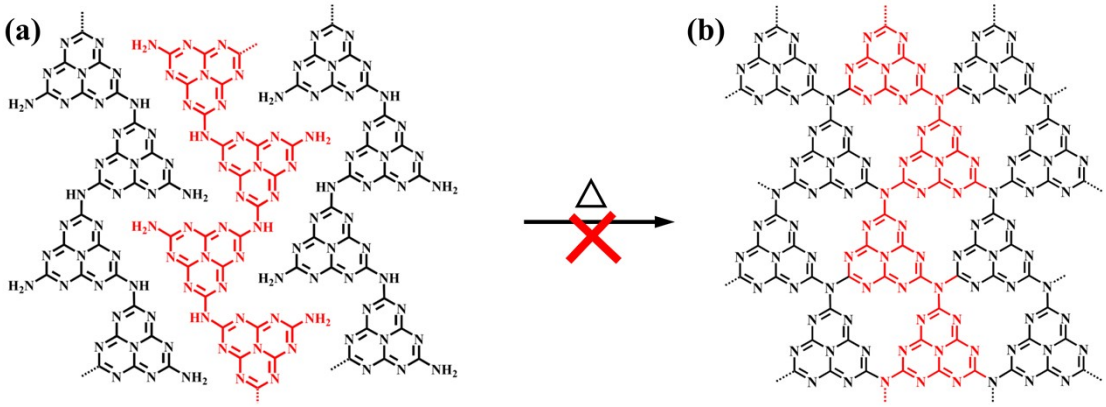

Fig. S1. The different structures of carbon nitride depicted in the contemporary literature: (a) 1D chains of heptazine and (b) a 2D framework of heptazine.

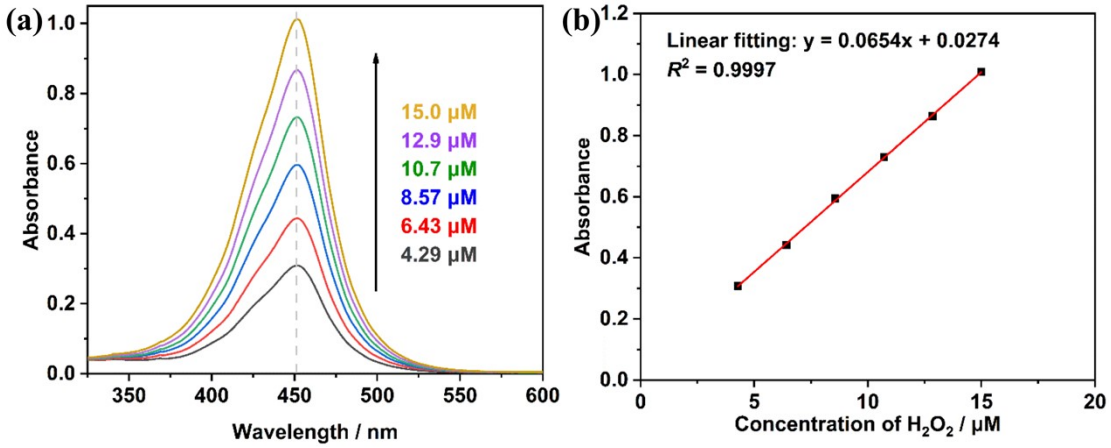

Fig. S2. (a) The standard spectra of the HRP/TMB solution with different concentration of H_2O_2. (b) The corresponding linear fitting: UV-vis absorption intensity at 450 nm vs. concentration of H_2O_2.

Table S2 Compositions and melting points of the metal salts for the synthesis of the samples.

Sample	Salt system	Composition [wt %]	Composition [mol %]	Melting point of salt system [°C]	Ref.
PTI	KCl/LiCl	55/45	41/59	352	S1
CN-70%	KCl/LiCl	70/30	57/43	532	S2
CN-80%	KCl/LiCl	80/20	70/30	626	S2
CN-90%	KCl/LiCl	90/10	84/16	706	S2
CN-100%	KCl	-	-	774	S1
BCN	-	-	-	-	-

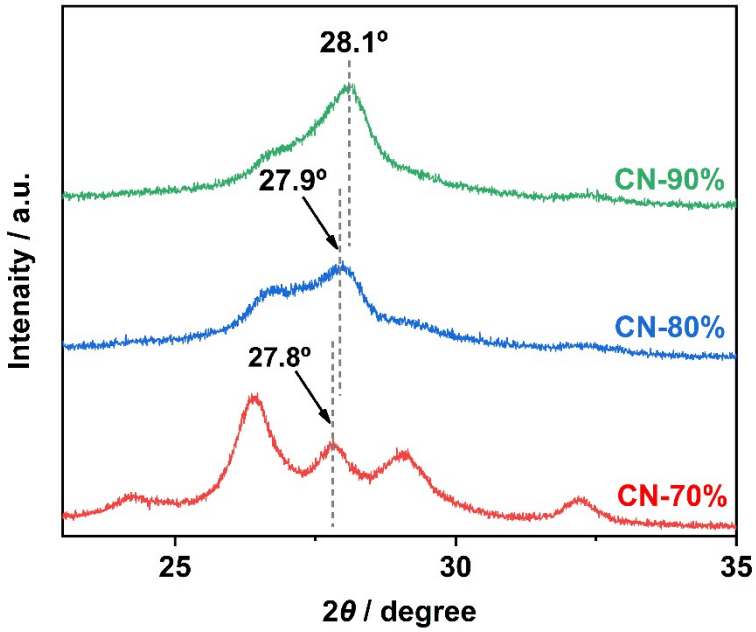

Fig. S3. Magnified images of XRD heptazine based (002) peaks for CN-70%, CN-80%, and CN-90%.

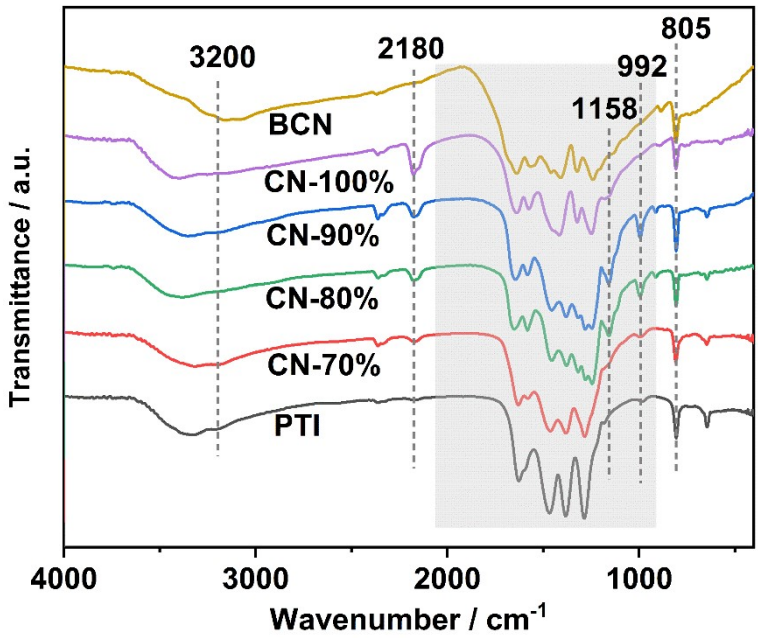

Fig. S4. FT-IR spectra of the prepared samples. The enlarged view in the range of 900-2100 cm^{-1} (marked by gray) are shown in Fig. 2b.

Table S3 Elemental compositions of the prepared samples, as determined by elemental analysis.

Sample	C [wt %]	N [wt %]	H [wt %]	**C/N molar ratio**
PTI	26.44	46.10	2.57	**0.67**
CN-70%	27.7	47.64	2.14	**0.68**
CN-80%	25.92	43.35	2.16	**0.70**
CN-90%	26.73	44.86	2.22	**0.70**
CN-100%	27.18	45.69	1.90	**0.69**
BCN	34.23	60.88	1.79	**0.66**

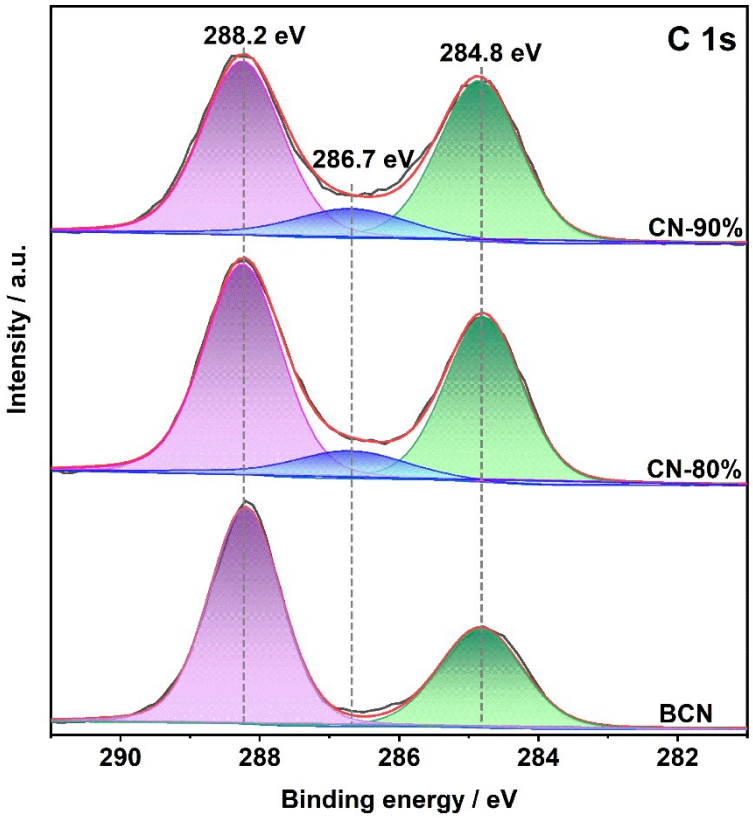

Fig. S5. XPS high-resolution C 1s spectra of BCN, CN-80%, and CN-90%.

Table S4 Relative ratios of different N species in CN-80%, CN-90%, and BCN, as determined by XPS spectra.

Sample	C–N=C [mol %]	$–NH_x$ [mol %]	$N–(C)_3$ [mol %]	**$N–(C)_3$/C–N=C molar ratio**
CN-80%	83.0	7.34	9.69	**0.117**
CN-90%	81.8	6.58	11.6	**0.142**
BCN	67.2	21.8	11.0	**0.163**

Table S5 The fitting parameters of the time-resolved transient photoluminescence decay curves for BCN, CN-80%, and CN-90%.

Sample	A_1 / %	τ_1 / ns	A_2 / %	τ_2 / ns	$\tau_{avg.}$ / ns
BCN	73.75	3.95	26.25	28.0	5.10
CN-80%	90.09	1.87	9.91	56.9	2.06
CN-90%	91.75	1.53	8.25	44.1	1.67

The emission decay curves of the samples were fitted by biexponential kinetics function (equation 1). The average PL lifetime (τ_{avg}) was deduced by the following equation 2：

$$I(t) = A_1\exp(-t/\tau_1) + A_2\exp(-t/\tau_2) \quad (1)$$

$$\tau_{avg} = \frac{A_1\tau_1^2 + A_2\tau_2^2}{A_1\tau_1 + A_2\tau_2} \quad (2)$$

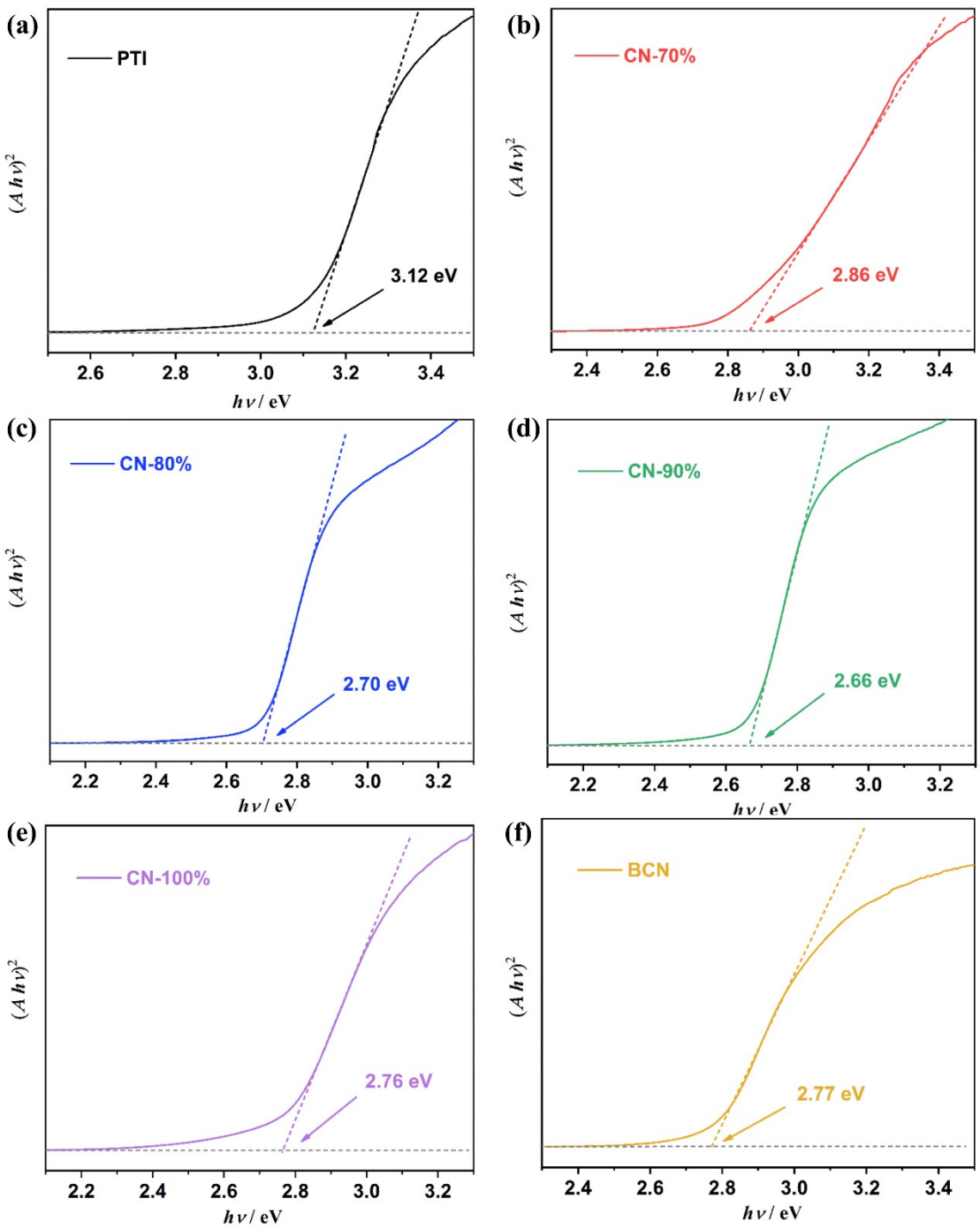

Fig. S6. Tauc plots of the prepared samples.

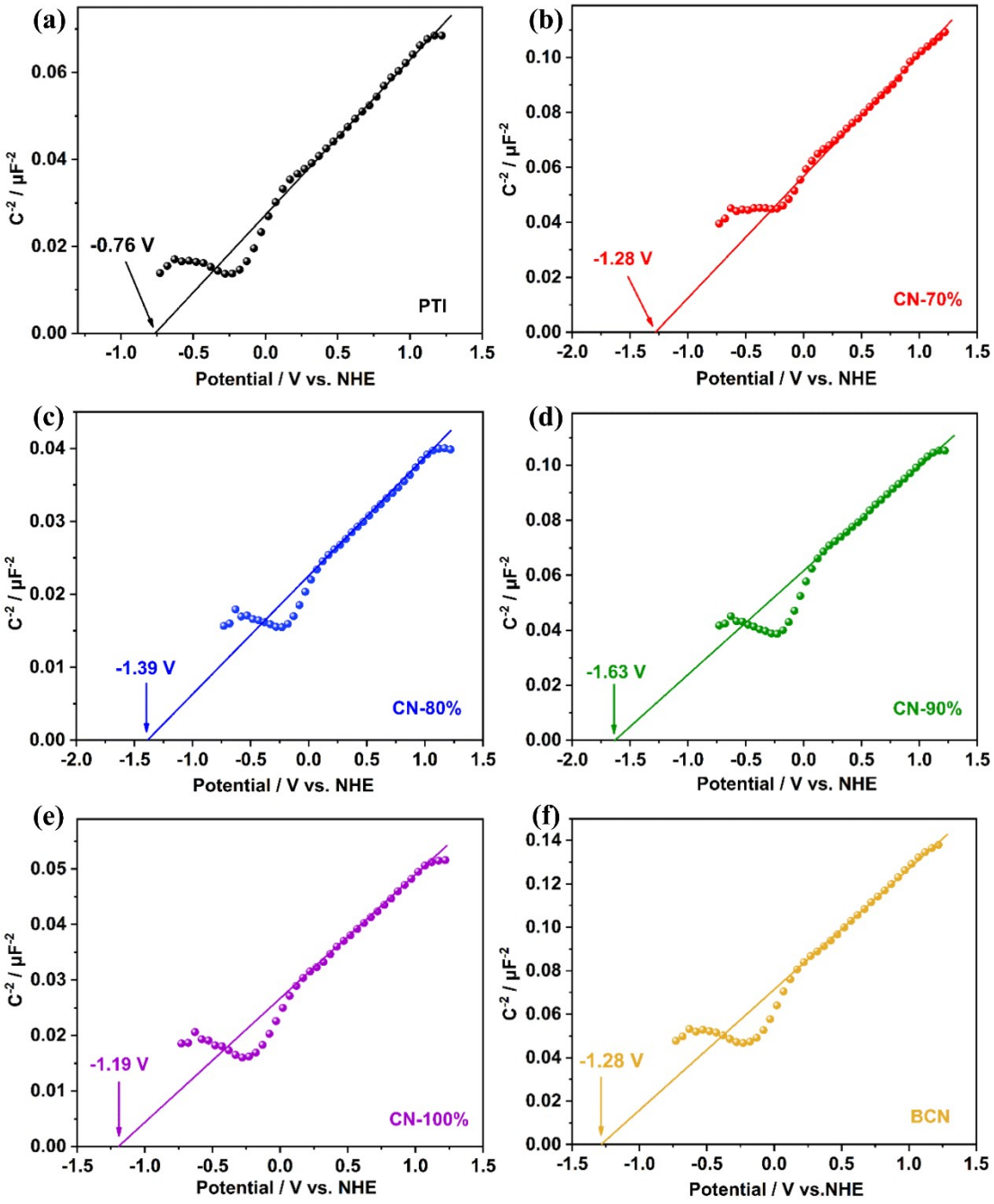

Fig. S7. Mott–Schottky curves of the prepared samples.

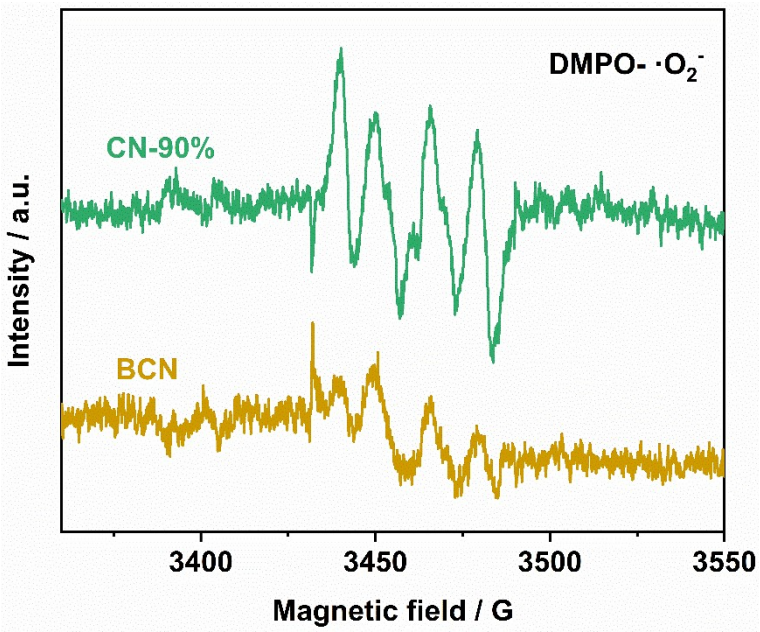

Fig. S8. ESR spectra of DMPO- $\bullet O_2^-$ for BCN and CN-90% suspensions under visible light irradiation.

Table S6 Comparison of AQE at 420 nm between this work and previous relevant studies.

molten salt	Method	AQE	Ref.
LiCl/KCl	post-calcination in molten salt	15[a]	S3
KCl	one-step calcination in molten salt	11.4	S4
KCl	post-calcination in molten salt	25.7[b]	S5
NaCl/KCl	one-step calcination in molten salt	24.8	S6
NaCl/KCl	post-calcination in molten salt	12	S7
LiCl/KCl	one-step calcination in molten salt	12.86	S8
NaCl/KCl	post-calcination in molten salt	9.9	S9
LiCl/KCl	**one-step calcination in molten salt**	**18.0**	**this work**

Note: The photocatalytic H_2 evolution reactions were carried out with Pt as the co-catalyst in the presence of sacrificial agent.

[a] the AQE of 57 % has been achieved in "sea water" (with additional 3 % NaCl).

[b] the AQE was achieved in "sea water" (with additional 3 % KCl).

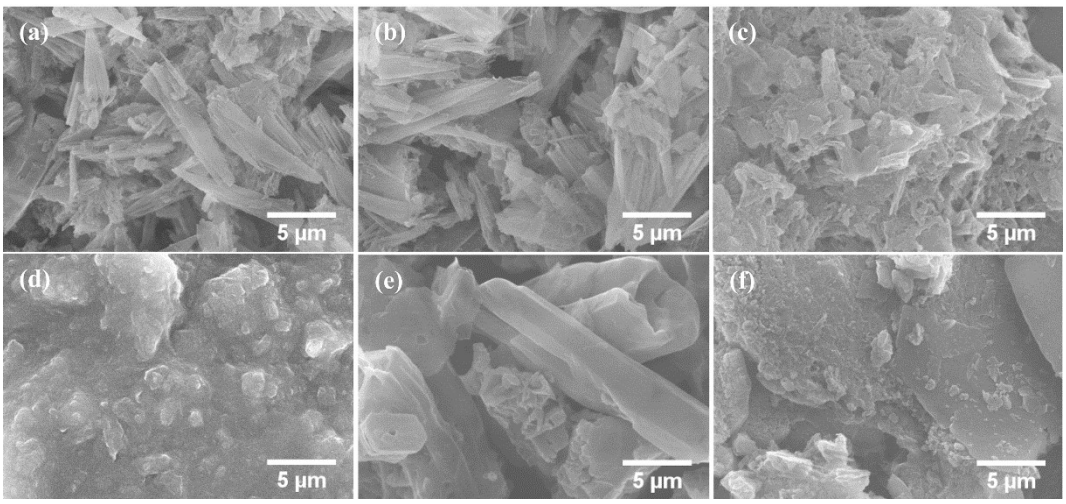

Fig. S9. SEM images of (a) PTI, (b) CN-70%, (c) CN-80%, (d) CN-90%, (e) CN-100%, and (f) BCN.

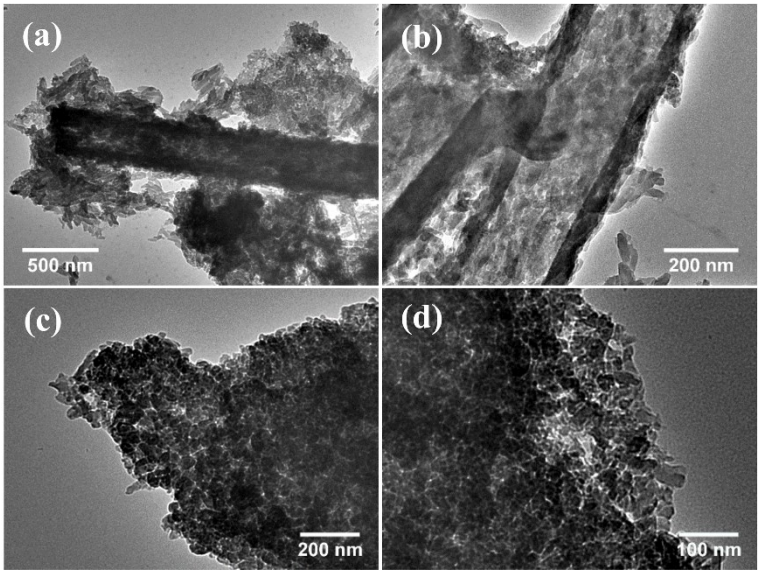

Fig. S10. TEM images of (a, b) CN-80% and (c, d) CN-90%.

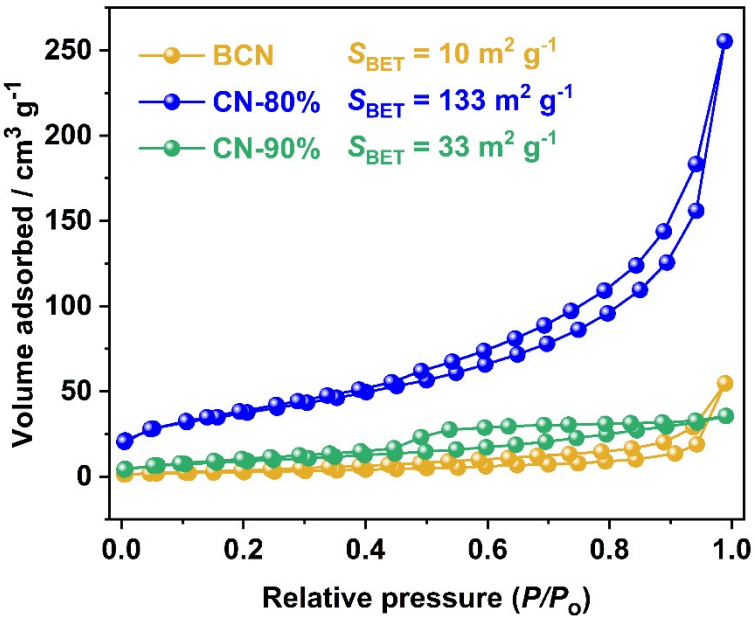

Fig. S11. N_2 adsorption and desorption isotherm curves of BCN, CN-80%, and CN-90%.

References

[S1] G. Zhang, L. Lin, G. Li, Y. Zhang, A. Savateev, S. Zafeiratos, X. Wang, M. Antonietti, Ionothermal synthesis of triazine–heptazine-based copolymers with apparent quantum yields of 60 % at 420 nm for solar hydrogen production from "sea water", Angew. Chem. Int. Ed. 57 (2018) 9372-9376.

[dataset] [S2] KCl-LiCl, 1 atm, data from FTsalt - FACT Salt databases, FactSage 8.2. https://www.crct.polymtl.ca/FACT/documentation/

[S3] G. Zhang, G. Li, Z. Lan, L. Lin, A. Savateev, T. Heil, S. Zafeiratos, X. Wang, M. Antonietti, Optimizing optical absorption, exciton dissociation, and charge transfer of a polymeric carbon nitride with ultrahigh solar hydrogen production activity, Angew. Chem. Int. Ed., 56 (2017) 13445-13449.

[S4] Y. Xu, X. He, H. Zhong, D.J. Singh, L. Zhang, R. Wang, Solid salt confinement effect: An effective strategy to fabricate high crystalline polymer carbon nitride for enhanced photocatalytic hydrogen evolution, Appl. Catal. B: Environ., 246 (2019) 349-355.

[S5] G. Zhang, Y. Xu, D. Yan, C. He, Y. Li, X. Ren, P. Zhang, H. Mi, Construction of K^+ ion gradient in crystalline carbon nitride to accelerate exciton dissociation and charge separation for visible light H_2 production, ACS Catal., 11 (2021) 6995-7005.

[S6] H. Zhang, F. Zheng, Z. Li, X. Cao, Z. Mou, S. Sun, J. Sun, L. Lang, Partially cross-linked carbon nitride with unimpeded charge transfer between different chains for boosting photocatalytic hydrogen production, Mater. Horiz., 10 (2023) 601-606.

[S7] M. Chang, Z. Pan, D. Zheng, S. Wang, G. Zhang, M. Anpo, X. Wang, Salt-melt synthesis of poly heptazine imides with enhanced optical absorption for photocatalytic hydrogen production, ChemSusChem, 16 (2023) e202202255.

[S8] S.-F. Ng, J.J. Foo, W.-J. Ong, Isotype heterojunction: tuning the heptazine/triazine phase of crystalline nitrogen-rich C_3N_5 towards multifunctional photocatalytic applications, Mater. Horiz., 11 (2024) 408-418.

[S9] T. Shi, X. Wang, X. Yu, G. Li, L. Wang, S. Li, J. Huang, A. Meng, Z. Li, Rational construction of carbon nitride homojunction photocatalyst for enhanced hydrogen evolution from water splitting, Energ. Convers. Manage., 300 (2024)

117941.